Differences in the Magnetic Properties of Co, Fe, and Ni 250−300 nm Wide Nanowires Electrodeposited in Amorphous Anodized Alumina Templates

Jian Qin,*,† Josep Nogués,‡ Maria Mikhaylova,† Anna Roig,§ Juan S. Muñoz,|| and Mamoun Muhammed*,†

Materials Chemistry Division, Royal Institute of Technology, SE 100 44 Stockholm, Sweden, Institució Catalana de Recerca i Estudis Avançats (ICREA) and Departament de Física, Universitat Autònoma de Barcelona, 08913 Bellaterra, Spain, Institut de Ciència de Materials de Barcelona (ICMAB-CSIC), Campus Universitat Autònoma de Barcelona (UAB), 08193 Bellaterra, Spain, and Departament de Física, Universitat Autónoma de Barcelona, 08913 Bellaterra, Spain

Received December 7, 2004. Revised Manuscript Received January 20, 2005

Anodized alumina membranes (AAMs) were synthesized by a *three-step* electrochemical anodization of aluminum. The anodization results in a hexagonally pseudo-ordered 2D array of nanochannels. The AAMs were used as templates to grow Ni, Co, and Fe nanowires, with diameters in the range of 250−300 nm, by electrodeposition. The AAM appears to be amorphous, while the metal nanowires are polycrystalline. The angular dependence of the coercivity, H_C, of the Ni nanowires presents a smooth variation from a $\mu_o H_C = 5.5$ mT when the field is applied perpendicular to the wires to $\mu_o H_C = 53$ mT when the field is applied parallel to them. However, the Co and Fe nanowires exhibit a peak in the angular dependence of H_C for fields applied close to the AAM plane (i.e., perpendicular to the wires). The competition between shape anisotropy and dipolar interactions between the nanowires seems to be responsible for the difference in magnetic behavior between the different metals.

1. Introduction

In recent years, there has been considerable interest in the fabrication of ferromagnetic nanostructures, both because of their fundamental properties and the wide range of possible applications.[1−3] Traditional methods based on lithography, e.g., electron beam, ion beam, or X-ray lithographies, are usually rather slow and costly.[1,4] One simple technique to obtain ordered arrays of nanostructures is using anodized alumina membranes (AAMs) as templates.[5−9] The templates are usually used to grow either nanowires by electrodeposition[10−12] or dots by evaporation.[13] This technique is inexpensive and convenient since it can be easily scaled up for industrial processing.[6] Actually, according to the method introduced by Masuda and Fukuda, a two-step anodization process of aluminum foils renders large areas of well-ordered porous membranes with narrow pore diameter distributions.[14] AAM templates have been widely used to study arrays of ferromagnetic nanowires since the simplicity to control parameters such as length, wire diameter, or interwire distance makes them an ideal playground to study a range of magnetic phenomena.[10−12] Moreover, possible applications such as magnetic recording media,[15] giant magnetoresistance,[16] or sensors[17] are also fueling the interest in these kinds of systems. For magnetic recording media applications the wire diameter and the interwire spacing should be as small as possible to increase the recording density; thus, most of the magnetic studies concentrate in sub-100-nm wires.[10−12] However, for other possible magnetic applications, such as those based on the magneto-optical[18] or microwave[19] proper-

* To whom correspondence should be addressed. Tel: +46 8 790 81 48. Fax: +46 8 790 90 72. E-mail: jian@mse.kth.se; mamoun@mse.kth.se.
† Royal Institute of Technology.
‡ ICREA and Departament de Física, Universitat Autònoma de Barcelona.
§ ICMAB-CSIC, Campus Universitat Autònoma de Barcelona.
|| Departament de Física, Universitat Autónoma de Barcelona.

(1) Martín, J. I.; Nogués, J.; Liu, K.; Vicent, J. L.; Schuller, I. K. *J. Magn. Magn. Mater.* **2003**, *256*, 449.
(2) Skomsky, R. *J. Phys.: Condens. Matter* **2003**, *15*, R841.
(3) Ross, C. A. *Annu. Rev. Mater. Sci.* **2001**, *31*, 203.
(4) (a) Yokoyama, Y.; Suzuki, Y.; Yuasa, S.; Ando, K.; Shigeto, K.; Shinjo, T.; Gogol, P.; Miltat, J.; Thiaville, A.; Ono, T.; Kawagoe, T. *J. Appl. Phys.* **2000**, *87*, 5618. (b) Schmitte, T.; Theis-Bröhl, K.; Leiner, V.; Zabel, H.; Kirsch, S.; Carl, A. *J. Phys.: Condens. Matter* **2002**, *14*, 7525.
(5) Whitney, T. M.; Jiang, J. S.; Searson, P.; Chien, C. L. *Science* **1993**, *261*, 1316.
(6) Shingubara, S. *J. Nanopart. Res.* **2003**, *5*, 17.
(7) Yin, A. J.; Li, J.; Jian, W.; Bennett, A. J.; Xu, J. M. *Appl. Phys. Lett.* **2001**, *79*, 1039.
(8) Bao, J.; Tie, C.; Xu, Z.; Ma, Q.; Hong, J.; Sang, H.; Sheng, D. *Adv. Mater.* **2002**, *14*, 44.
(9) Steinhart, M.; Wendorff, J. H.; Greiner, A.; Wehrspohn, R. B.; Nielsch, K.; Schilling, J.; Choi, J.; Gösele, U. *Science* **2002**, *296*, 1997.
(10) Sellmyer, D. J.; Zheng, M.; Skomski, R. *J. Phys.: Condens. Matter* **2001**, *13*, R433.
(11) Routkevitch, D.; Tager, A. A.; Haruyama, J.; Almawlawi, D.; Moskovits, M.; Xu, J. M. *IEEE Trans. Electron Dev.* **1996**, *43*, 1646.
(12) Li, C. Z.; Lodder, J. C. *J. Magn. Magn. Mater.* **1990**, *88*, 236.
(13) Liu, K.; Nogués, J.; Leighton, C.; Masuda, H.; Nishio, K.; Roshchin, I. V.; Schuller, I. K. *Appl. Phys. Lett.* **2002**, *81*, 4434.
(14) Masuda, H.; Fukuda, K. *Science* **1995**, *268*, 1466.
(15) (a) Kawai, S.; Ishiguro, I. *J. Electrochem. Soc.* **1976**, *123*, 1047. (b) Qin, D. H.; Lu, M.; Li, H. L. *Chem. Phys. Lett.* **2001**, *350*, 51.
(16) (a) Liu, K.; Nagodawithana, K.; Searson, P. C.; Chien, C. L. *Phys. Rev. B* **1995**, *51*, 7381. (b) Evans, P. R.; Yi, G.; Schwarzacher, W. *Appl. Phys. Lett.* **2000**, *76*, 481.
(17) Basu, S.; Chatterjee, S.; Saha, M.; Bandyopadhyay, S.; Mistry, K.; Sengupta, K. *Sens. Actuators, B* **2001**, *79*, 182.
(18) Melle, S.; Menéndez, J. L., Armelles, G.; Navas, D.; Vázquez, M.; Nielsch, K.; Wehrspohn, R. B.; Gösele, U. *Appl. Phys. Lett.* **2003**, *83*, 4547.

10.1021/cm047870q CCC: $30.25
Published on Web 02/25/2005

ties of the arrays, larger wire diameters may be more appealing. Nevertheless, studies of arrays of nanowires, grown in AAM, with diameters above 200 nm are rather scarce.[19−24]

In this study, we present the synthesis of alumina membranes by a *three-step* anodization process, which were subsequently used as templates to grow arrays of Ni, Fe, and Co nanowires with 250−300 nm diameter and 3−8 μm length. Although the Ni, Fe, and Co nanowires exhibit a clear uniaxial anisotropy, with the easy axis along the wires, the detailed angular dependence of the coercivity of Fe and Co nanowires is rather complex, related to magnetization reversal by curling. In contrast, the coercivity of Ni changes smoothly with angle. This arises from the weaker uniaxial shape anisotropy of the Ni wires, due to their lower saturation magnetization, making them more sensitive to the effects of interwire interactions.

2. Experimental Methods

Chemicals. The aluminum foil was 99.9% pure and supplied by Merck (Germany). Cobalt sulfate ($CoSO_4 \cdot 7H_2O$ > 99%), ferrous sulfate ($FeSO_4 \cdot 7H_2O$ > 99%), chromium(VI) oxide (CrO_3 > 99%), oxalic ($H_2C_2O_4$ > 99%), boric (H_3BO_3 > 99%), perchloric ($HClO_4$ ~ 65%), and ascorbic acids ($C_6H_8O_6$ > 99%) were purchased from Sigma Aldrich chemicals. Sodium hydroxide (NaOH > 99%) was obtained from KEBO chemicals (Sweden). Nickel sulfate ($NiSO_4 \cdot 6H_2O$ > 99%) and nickel chloride ($NiCl_2 \cdot 6H_2O$ > 99%) were purchased from MERCK and KEBO, respectively. All organic solvents were analytical grade, and water was purified by the Milli-Q system.

Synthesis of the AAMs. In this study, AAMs were produced by a three-step anodization process. A 99.9% pure Al foil was pretreated by annealing it at 500 °C for 4 h in order to release mechanical stress and subsequently electropolishing it in a mixture of C_2H_5OH and $HClO_4$ (65%) to smoothen the surface. The first step of anodization was carried out in an electrolyte of 0.3 M $H_2C_2O_4$ at 100 V_{DC} for 2 h at 4 °C under a mild agitation. Subsequently, the formed Al_2O_3 membrane was etched away in an acidic mixture of 5% H_3PO_4 and 1.8% H_2CrO_4 at 60 °C for 30 min. The Al foil, with a fresh surface, was re-anodized for 2 h under the same conditions as the first anodization step. Upon completion of the second anodization step, the Al−Al_2O_3 system was anodized in a mixture of acetone and $HClO_4$ (1:1 volume ratio), at 110 V_{DC}, for an additional 5 min to break the Al_2O_3 barrier layer at the bottom of the anodized channels. This process also detaches almost completely the AAM from the Al foil. Finally, to ensure that the prepared AAMs had through channels, a 5% H_3PO_4 etch was applied at 40 °C for 10 min to completely remove the remaining barrier layer at the bottom of the channels. This treatment with H_3PO_4 also etches away part of the walls of the channels, hence widening the pores as well.

Electrodeposition of Ni, Co, and Fe Nanowires. To perform the metal electrodeposition inside AAMs channels, one side of the membrane was coated by a thin layer of DC-sputtered gold to obtain a conducting layer at the bottom of the pores, which acted as a counter electrode. The electrodeposition was controlled by Model 366A, Bi-Potentiostat (Princeton Applied Research). The nanowires were grown inside the AAMs using a potentiostatic electrodeposition procedure. A Watts-type electrolyte ($NiSO_4 \cdot 6H_2O$, 300 g/L; $NiCl_2 \cdot 6H_2O$, 45 g/L; H_3BO_3, 45 g/L) was used as an electroplating solution to fabricate Ni nanowires.[25] The pH value was maintained at 4.0. The electrolysis was carried out at 25 °C, 2.0 V_{DC} for 15 min. Co nanowires were deposited by using a solution with a mixture of 140 g/L $CoSO_4$ and 50 g/L H_3BO_3 at 25 °C, 2.5 V_{DC} for 1.5 h.[8] Electrodeposition of Co nanowires was undertaken at pH 4.0. Fe nanowires were electrodeposited by using an electrolyte containing 120 g/L $FeSO_4 \cdot 7H_2O$, a small amount of ^{57}Fe-enriched $FeCl_3$, 45 g/L H_3BO_3, and 1 g/L ascorbic acid at 25 °C, 2.0 V_{DC} for 10 min.[26] The pH of the solution during electrodeposition of Fe nanowires was kept at 2.0. Note that no capping of the nanowires was undertaken. After the electrodeposition process, the AAMs, with metal wires embedded inside, were carefully cleaned by acetone for further physicochemical characterization.

Characterizations. X-ray diffraction (XRD) patterns of the AAMs and the nanowires were recorded by a PHILIPS-PW1830 system using a monochromatized X-ray beam with a nickel-filtered Cu Kα radiation. Scanning electron microscopy (SEM) images of the AAMs and the metal nanowires were taken by a scanning electron microscope (JEOL JSM-840 model), equipped with energy-dispersive X-ray analysis (EDX). The magnetic measurements were carried out at room temperature using a vibrating sample magnetometer (VSM) with a maximum applied field of 12 kOe. The measurements of hysteresis loops were performed at different angles between the applied field and the long axis of the wires. Mössbauer spectra (MS) were acquired at room temperature, with the γ-rays applied along the wire axis, using a conventional Mössbauer spectrometer with a ^{57}Co/Rh source for which velocity calibration was done using a 25 μm foil of metallic iron.

3. Results and Discussion

Figure 1a shows the SEM image of an AAM with average pore diameter of about 250 nm, thickness of 80 μm (Figure 1b), and pore density of about $1 \times 10^9/cm^2$ (i.e., center-to-center distance of about $s \sim 420$ nm). As can be seen from the SEM image of the backside of the AAM without the additional acetone-$HClO_4$ anodization (Figure 1c), a highly packed spherical shape structure of the AAM is observed; i.e., the channels remain closed. However, if the extra anodization is performed, the bottom of the pores partially open (Figure 1d), which eases further processing. Etching by 5% H_3PO_4 causes the formation of AAM with through channels and the widening of the pores (Figure 1e). Using the extra additional acetone-$HClO_4$ anodization, AAMs with a high ratio of through channels could be prepared without destroying the AAMs by over-etching, as can occur when applying only acid-etching to open the pores.[14] From Figure 1a it can be seen that although the AAMs present a local hexagonal pore arrangement, the long-range order of the

(19) Encinas-Oropesa, A.; Demand, M.; Piraux, L.; Huynen, I.; Ebels, U. *Phys. Rev. B* **2001**, *63*, 104415.
(20) (a) Lederman, M.; O'Barr, R.; Schultz, S. *IEEE Trans. Magn.* **1995**, *31*, 3793. (b) O'Barr, R.; Schultz, S. *J. Appl. Phys.* **1997**, *81*, 5458. (c) O'Barr, R.; Lederman, M.; Schultz, S.; Xu, W.; Scherer, A.; Tonuci, R. J. *J. Appl. Phys.* **1996**, *79*, 5303.
(21) Cao, H.; Tie, C.; Xu, Z.; Hong, J.; Sang, H. *Appl. Phys. Lett.* **2001**, *78*, 1592.
(22) García, J. M.; Asenjo, A.; Velázquez, J.; García, D.; Vázquez, M.; Aranada, P.; Ruiz-Hitzky, E. *J. Appl. Phys.* **1999**, *85*, 5480.
(23) Raposo, V.; Garcia, J. M.; González, J. M.; Vázquez, M. *J. Magn. Magn. Mater.* **2000**, *222*, 227.
(24) Lin, S. W.; Chang, S. C.; Liu, R. S.; Hu, S. F.; Jan, N. T. *J. Magn. Magn. Mater.* **2004**, *282*, 28.
(25) Nielsch, K.; Wehrspohn, R. B.; Barthel, J.; Kirschner, J.; Gösele, U.; Schweinboeck, T.; Weiss, D.; F. Fischer, S.; Kronmüller, H. *J. Magn. Mater. Magn.* **2002**, *249*, 234.
(26) AlMawlawi, D.; Coombs, N.; Moskovits, M. J. *Appl. Phys.* **1991**, *70*, 4421.

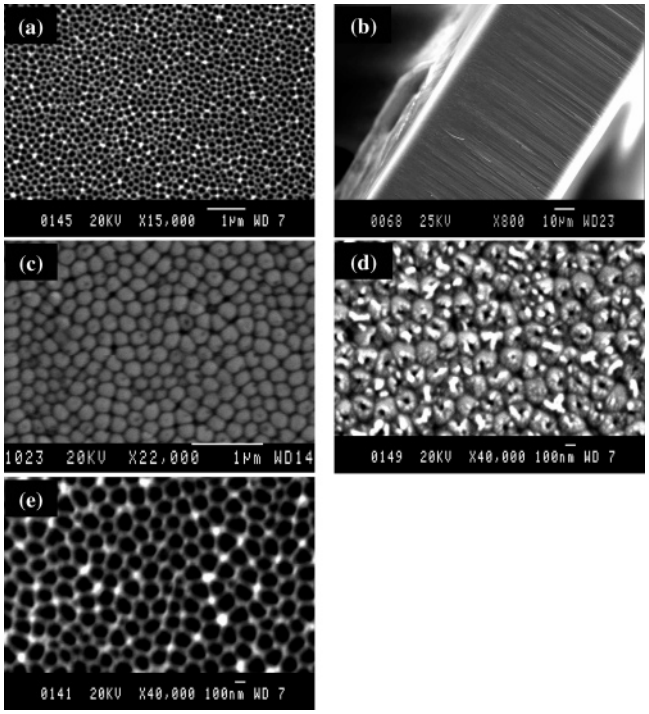

Figure 1. SEM images of AAM: (a) front side of AAM; (b) cross section of AAM; (c) backside of AAM; (d) backside of the AAM after the third anodization step; (e) backside of the AAM after additional etching in phosphoric acid.

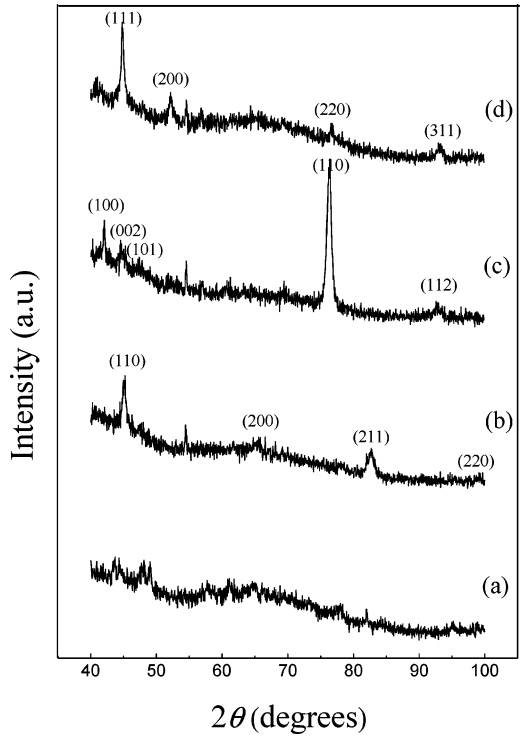

Figure 2. XRD patterns of (a) AAM, (b) Fe, (c) Co, and (d) Ni nanowires. The peaks for the Fe, Co, and Ni were indexed using bcc, hcp, and fcc structures.

pores is rather limited. Nevertheless, usually the ordered domains can reach several μm (Figure 1e).

The XRD of the as-prepared AAM (Figure 2a) shows an amorphous (or nanocrystalline) structure. Traditionally, the AAMs are annealed before being used as templates to crystallize them,[27] thus avoiding the possibility of irregular growth of the nanowires in the amorphous AAMs.[28] In this study, we have utilized as-anodized, *amorphous*, AAMs as templates for the electrodeposition of the metal nanowires.

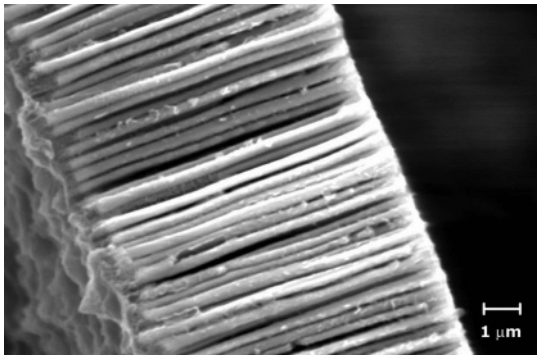

Figure 3. SEM image of cross section of Co nanowires.

Table 1. Summary of the Geometrical Characteristics, Length (*l*), Average Diameter (*d*), and Center-to-Center Distance between Pores (*s*), of the Ni, Co, and Fe Nanowires

	l (μm)	d (nm)	s (nm)
Ni	4.5	280	380
Co	8.1	320	410
Fe	3.2	250	420

Shown in Figure 3 is the SEM image of Co nanowires after the membrane has been etched away by 1 M NaOH. It can be clearly seen that the wires grow highly homogeneous in shape, with the same length, and parallel to each other. Moreover, top view images (data not shown) demonstrate that the local 2D hexagonal order of the AAMs is maintained in the wires. The analysis of the images of different wires confirms that wire diameters coincide with the pore diameter. A summary of the geometry of the three systems is given in Table 1. Note also that the composition of the wires was confirmed to be Ni, Co, and Fe by EDX (data not shown).

Figure 2b−d depicts the XRD patterns of Fe, Co, and Ni nanowires embedded inside porous AAM. From the XRD patterns it can be inferred that Fe and Ni grow in their bcc and fcc crystal structures, respectively, and are clearly polycrystalline. However, Co grows hcp and exhibits a weak (110) texture. It is noteworthy that Fe and Co are often found to grow strongly textured inside AAMs.[29,30] The fact that the wires are polycrystalline may be related to the wider diameter of the pores, the amorphous nature of the AAMs, or the electrodeposition process.

Shown in Figure 4 are the hysteresis loops of the Fe, Co, and Ni nanowires for fields applied parallel and perpendicular to the wire axis. It can be seen, for the three systems, that when the field is applied perpendicular to the wires, the hysteresis loop exhibits a small coercivity, H_C, a small

(27) (a) Wang, Y. C.; Leu, I. C.; Hon, M. H. *J. Appl. Phys.* **2004**, *95*, 1444. (b) Mardilovich, P.; Routkevitch, D.; Govyadinov, A. *Microfabricated systems and MEMS V.;* Hesketh, P. J., Ang, S. S., Bailey, W. E., Davidson, J. L., Hughes, H. G., Misra, D., Eds.; Electrochemical Society: Pennington, 2000; Vol. 2000−19, p 33.
(28) Gras, R. Master Degree Thesis, Royal Institute of Technology, Stockholm, Sweden, 2004, ISRN KTH/MSE- -04/49- -SE+CHEM/EX.
(29) (a) Yang, S.; Zhu, H.; Yu, D.; Jin, Z.; Tang, S.; Du, Y. *J. Magn. Magn. Mater.* **2000**, *222*, 97. (b) Zhang, X. Y.; Wen, G. H.; Chan, Y. F.; Zheng, R. K.; Zhang, X. X.; Wang, N. *Appl. Phys. Lett.* **2003**, *83*, 3341.
(30) (a) Khan, H. R.; Petrikowski, K. *Mater. Sci. Eng. C* **2002**, *19*, 345. (b) Khan, H. R.; Petrikowski, K. *J. Magn. Magn. Mater.* **2002**, *249*, 458.

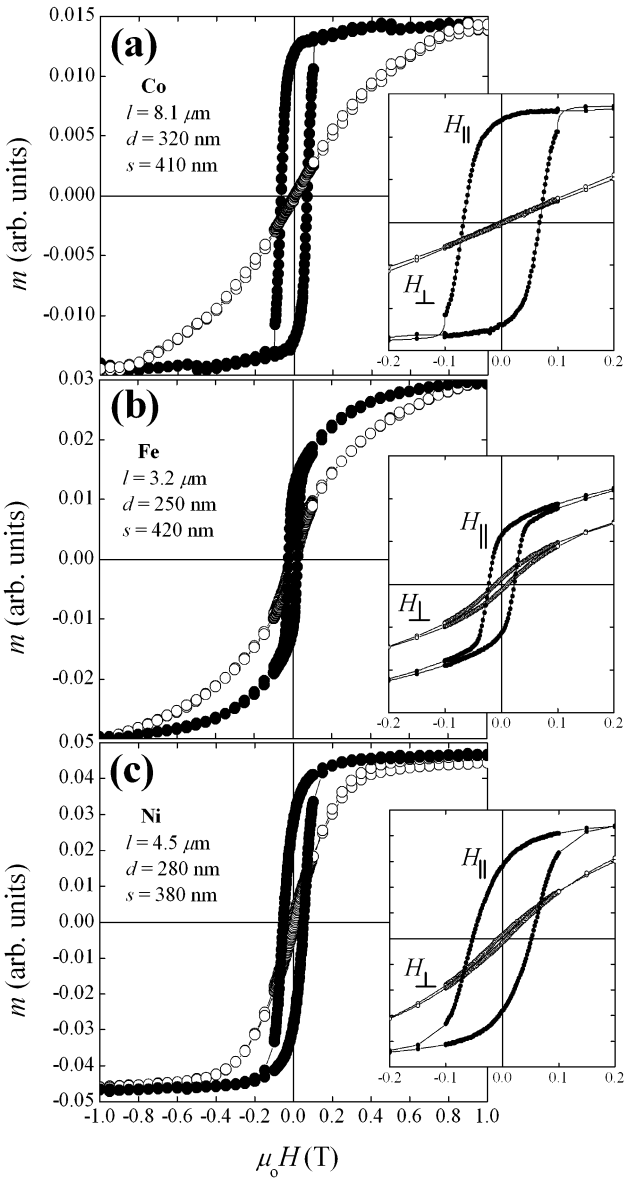

Figure 4. Hysteresis loops of the (a) Co, (b) Fe, and (c) Ni nanowires for fields applied parallel, $H_{||}$ (filled symbols), and perpendicular, $H_{\perp}$ (open symbols), to the wire axis. The insets are low-field enlargements of the hysteresis loops.

remanence, M_R, and large saturation field (i.e., the field necessary to reach the saturation magnetization, M_S). Contrarily, when the field is applied parallel to the wires, H_C and M_R become larger and the different systems reach M_S at rather low fields. This is the behavior typical of a hard and easy axis hysteresis loop, respectively.[31] Hence, this indicates that the easy axis of the system is along the wires for all three systems. This is characteristic of polycrystalline wires where the shape anisotropy dominates over the intrinsic magnetocrystalline anisotropy, K_{MC}, and thus dictates the magnetic behavior of the system. The shape anisotropy is given by $K_{SH} = \mu_o(1 - 3N)(M_S)^2/4$, where μ_o is the permeability of vacuum and N is the demagnetizing factor. Since the aspect ratio, l/d (length/diameter), is rather large, the demagnetizing factor is almost zero for all three wires. Hence, the infinite cylinder approximation for the shape

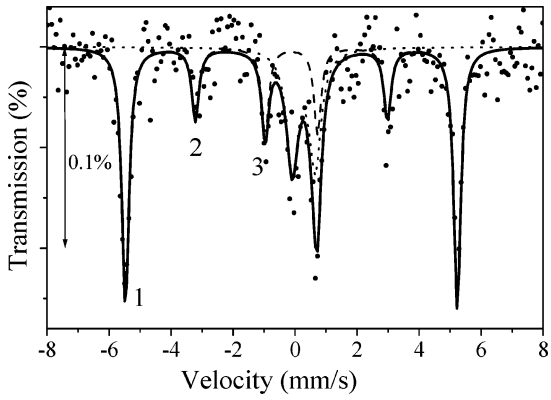

Figure 5. Mössbauer spectrum of the Fe nanowires obtained at room temperature. The continuous lines are a fit to the data using a sextet for Fe (dashed line) and a doublet for the paramagnetic component (dotted line). The peak numbers (1,2,3) for the Fe sextet are indicated.

anisotropy $K_{SH} = \mu_o(M_S)^2/4$ is appropriate in this case. Moreover, the anisotropy field, $\mu_o H_K$, i.e., the field needed to saturate the hysteresis loops in the hard axis, i.e., perpendicular to the wires, increases from about $\mu_o H_K$(Ni) $\sim$ 0.3 T to $\mu_o H_K$(Co) $\sim$ 0.9 T and $\mu_o H_K$(Fe) $\sim$ 1.0 T. This is in a good agreement with what would be expected from a simple Stoner-Wolfarth theory,[32] where $\mu_o H_K = 2\ K/M_S$, which for the shape anisotropy becomes $\mu_o H_K = \mu_o M_S/2$, i.e., $\mu_o H_K = 0.31$, 0.905, and 1.075 T for Ni, Co, and Fe, respectively.

It is noteworthy that Fe and Co nanowires often exhibit easy axes either perpendicular to the wires or at an angle to the wire axis. This is actually linked to the textured growth of the wires since in such cases K_{MC} may be of the same order as, or even dominate, K_{SH}.[33] In our case, since the wires are polycrystalline, the average magnetocrystalline anisotropy is reduced over the nominal K_{MC}; hence, $K_{SH} \gg K_{MC,aver}$.

The easy axis direction of the Fe nanowires is confirmed, by Mössbauer spectroscopy, to be roughly along the wire axis. In Figure 5 it can be seen for the magnetically blocked component, corresponding to metallic Fe, that the ratio of the intensities of the peaks 2 and 3, $R_{2,3} = I_2/I_3$, is about $R_{2,3} \sim 0.7$. For the magnetization parallel or perpendicular to the γ-rays, the $R_{2,3}$ ratio becomes, $R_{2,3}(||) = 0$ and $R_{2,3}(\perp) = 4$, respectively.[34] Consequently, for the Fe nanowires the magnetization appears to be closer to the parallel to the γ-rays, i.e., along the wire axis. The fact that $R_{2,3} > 0$ is consistent with the fact that $M_R < M_S$. Moreover, the Mössbauer spectrum indicates the presence of a paramagnetic component at room temperature, which could be attributed to an iron oxide. This oxide is probably due to partial oxidation of the wires since the wires were not capped. This is in agreement with the hysteresis loops, which exhibit a component which is difficult to saturate (i.e., paramagnetic); i.e., they exhibit a strong curvature of the easy axis loop.

To gain further insight into the magnetic behavior of the three systems, the angular dependence of the hysteresis loops

(31) Cullity, B. D. *Introduction to Magnetic Materials*; Addison-Wesley Publ.: Reading, 1972.

(32) Stoner, E. C.; Wohlfarth, E. P. *Trans. R. Soc. London* **1948**, *240*, 599.

(33) Henry, Y.; Ounadjela, K.; Piraux, L.; Dubois, S.; George, J. M.; Duvail, J. L. *Eur. Phys. J. B* **2001**, *20*, 35.

(34) (a) Zhan, Q. F.; He, W.; Ma, X.; Liang, Y. Q.; Kou, Z. Q.; Di, N. L.; Cheng, Z. H. *Appl. Phys. Lett.* **2004**, *85*, 4690. (b) Fagg, L. W.; Hanna, S. S. *Rev. Mod. Phys.* **1959**, *31*, 711.

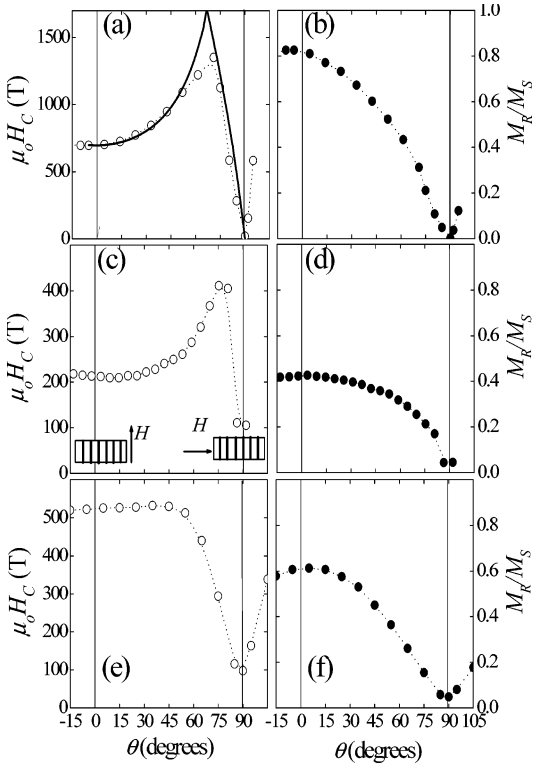

Figure 6. Angular dependence of the coercivity, H_C (open symbols), and squareness, M_R/M_S (filled symbols), for Co (a,b), Fe (c,d), and Ni (e,f) nanowires. The continuous line in (a) is a simulation of a curling reversal, while the dashed lines are guides to the eye. Given in (c) is the measurement geometry.

was measured. Shown in Figure 6 is the angular dependence of H_C and the squareness, M_R/M_S for the three systems. M_R/M_S exhibits a similar behavior for Fe, Co, and Ni, decreasing smoothly from a maximum value for fields applied parallel to the wires to almost zero for fields applied perpendicular to them. However, the squareness values are maximum for Co with $M_R/M_S > 0.8$ and decrease to $M_R/M_S \sim 0.6$ for Ni and finally become $M_R/M_S \sim 0.4$ for Fe. The low values for Fe are probably due to the contribution of the iron oxide component to the total magnetization, which increases M_S but does not contribute to M_R. The lower M_R/M_S for Ni could be due to dipolar interactions since it is well-known that such interactions tend to shear the hysteresis loops in interacting systems[1−3] and in particular in arrays of nanowires,[23,35,36] although other effects, such as the disorder in the 2D arrangement of the nanowires,[36] the distribution of coercivities of the individual wires[36] or the magnetization state of the nanowire certainly plays a role (see below).

Remarkably, the angular dependence of H_C for Co and Fe display a nonmonotonic behavior. Namely, the coercivity increases with increasing angle, reaching a maximum for angles close to $H_\perp$ ($\theta \sim 70-75°$) and rapidly dropping to almost $H_C \sim 0$ at $H_\perp$. As can be seen in Figure 6, the drop in H_C occurs in a very narrow angle range. Contrarily, the angular dependence of H_C for Ni is smooth, being roughly constant at the maximum H_C for a range of angles and finally decreasing to almost zero at $H_\perp$.

To find the origin of this different behavior, we will analyze qualitatively the reversal of the nanowires. Since the width of the wires is rather large, they cannot be in a single domain state. Actually, according to the magnetic phase diagram of cylinders, given the aspect ratio of the wires studied, they should be in a vortex state.[37] This could explain, in part, the reduced M_R observed for all the systems since vortex states are known to have reduced magnetization in zero field.[35,38] Moreover, simulations show that although wide wires reverse their magnetization by vortex nucleation, several of the features observed during magnetization reversal are similar to the ones observed for curling type of reversal. In particular, the angular dependence of the coercivity has been found to be analogous in both types of reversals, although in the case of vortex formation the critical volume is smaller than the physical volume of the wire.[39,40] The theoretical angular dependence of H_C for wires of different widths has been extensively studied using coherent rotation and curling mechanisms.[20,41,42] For curling it has been found that the angular dependence of the coercivity depends strongly on the ratio $S = r/r_o$, where r is the radius of the wire and r_o is the exchange length.[43] The angular dependence is given by $H_C = 1.08(1 - 1.08S^{-2})/S^2[(1 - 1.08S^{-2})^2 - \sin^2\theta(1 - 2.16S^{-2})]^{1/2}$, for a range of angles, which depends on r/r_o, reverting to coherent rotation for high enough angles.[43]

As can be seen in Figure 6a, the simulation of the curling reversal, with $S = 3$, agrees qualitatively with the experimental data of the Co nanowires. For a better agreement effects such as distribution of radii or interactions should be taken into account. Nevertheless, a value of $S = 3$, assuming $r_o = 5$ nm for Co, would imply a wire diameter of 30 nm, i.e., much smaller than the real wire diameter. This is in agreement with theoretical studies[39,40] and measurements of the switching fields of *isolated* Ni wires diameters in the range of 300 nm, where exceedingly small values of r_o were found.[20]

The angular dependence of H_C for Ni cannot be explained using simple curling or coherent rotation reversal modes. However, it has been found theoretically that dipolar interactions alter the magnetic properties of the wires[44] and,

(35) Ross, C. A.; Hwang, M.; Shima, M.; Cheng, J. Y.; Farhoud, M.; Savas, T. A.; Smith, H. I.; Schwarzacher, W.; Ross, F. M.; Redjdal, M.; Humphrey, F. B. *Phys. Rev. B* **2002**, *65*, 144417.
(36) (a) Vázquez, M.; Hernández-Vélez, M., Pirota, K.; Asenjo, A.; Navas, D.; Velásquez, J.; Vargas, P.; Ramos C. *Eur. Phys. J. B* **2004**, *40*, 489. (b) Vázquez, M.; Nielsch, K.; Vargas, P.; Velázquez, J.; Navas, D.; Pirota, K.; Hernández-Vélez, M.; Vogel, E.; Cartes, J.; Wehrspohn R. B.; Gösele U. *Physica B* **2004**, *343*, 395.
(37) (a) Metlov K. L.; Guslienko, K. Y. *J. Magn. Magn. Mater.* **2002,** *242−245*, 1015. (b) Scholz, W.; Guslienko, K. Y.; Novosad, V.; Suess, D.; Schrefl, T.; Chantrell, R. W.; Fidler, J. *J. Magn. Magn. Mater.* **2003**, *266*, 155. (c) Skidmore, G. D.; Kunz, A.; Campbell, C. E.; Dahlberg, E. D. *Phys. Rev. B* **2004**, *70*, 012410.
(38) Vortex type states in high aspect ratio wires are known to have reduced remanence. Although contrary to in-plane vortex (which exhibit zero remanence), the remanence in wire-type systems can be significant.
(39) Ferré, R.; Ounadjela, K.; George, J. M.; Piraux, L.; Dubois, S. *Phys. Rev. B* **1997**, *56*, 14066.
(40) Schabes, M. E.; Bertram, H. N. *J. Appl. Phys.* **1988**, *64*, 5832.
(41) (a) Wernsdorfer, W.; Doudin, B.; Mailly, D.; Hasselbach, K.; Benoit, A.; Meier, J.; Ansermet, J. P.; Barbara, B. *Phys. Rev. Lett.* **1996**, *77*, 1873. (b) Zhu, H.; Yang, S., Ni, G.; Yu, D.; Du, Y. *J. Magn. Magn. Mater.* **2001**, *234*, 454.
(42) (a) Huysmans, G. T. A.; Lodder, J. C.; Wakui, J. *J. Appl. Phys.* **1988**, *64*, 2016. (b) Lodder, J. C.; Li, C. Z. *IEEE Trans. Magn.* **1989**, *25*, 4171.
(43) (a) Shtrikman, S.; Treves, D.; *J. Phys. Radium* **1959**, *20*, 286. (b) McCurrie, R. A.; Jackson, S. *IEEE Trans. Magn.* **1980**, *16*, 1310.

in particular, the angular dependence of H_C.[42,45] For example, it was found that interactions rapidly reduce the sharp features in H_C close to $H_\perp$ in the curling mode, resulting in a smooth variation of H_C with angle, in qualitative agreement with the experimental angular dependence of the Ni wires.

Actually, when the dipolar field of the neighboring wires is of the order of the anisotropy field, the interactions can start to influence the magnetization behavior of the wires, e.g., coercivity or remanence, and in particular their angular dependence. This effect will probably be most significant for Ni, which has the smallest anisotropy field. We can estimate the dipolar field, in first approximation, by evaluating the field created by a dipole of length l, i.e., the length of the wire, at a distance s, i.e., the center-to-center distance, where s is small compared to l: $\mu_o H_d = m/[s^2 + (l^2/4)]^{3/2}$, where m is the magnetic moment of the wire, which is $m = M_S(\pi l r^2)$.[31] Using the values in Table 1 for Ni, we obtain, for one wire, $\mu_o H_d = 0.015$ T. Taking into account that each wire has 6 neighbors and that the dipolar interaction is long ranged by the dipolar field, we can approximate $\mu_o H_{d,tot} \sim 9\mu_o H_d = 0.13$ T, which is indeed close to the anisotropy field of the Ni wires ($\mu_o H_K = 0.3$ T). Moreover, since the interwire distance is much smaller than the length, higher order terms in the interaction field should be taken into account,[46] which could further increase $\mu_o H_d$. Hence, due to the interactions, groups of wires could actually have a cooperative reversal; thus, their magnetic properties cannot be analyzed by models of individual wires and should be evaluated as a whole. Consequently, interactions seem a plausible cause for the difference in angular dependence of the coercivity of the Ni nanowires.

(44) Porrati, F.; Huth, M. *Appl. Phys. Lett.* **2004**, *85*, 3157.
(45) Hertel, R. *J. Appl. Phys.* **2001**, *90*, 5752.
(46) Velázquez, J.; Pirota, K. R.; Vázquez, M. *IEEE Trans. Magn.* **2003**, *39*, 3049.

4. Conclusions

Anodized alumina membranes (AAMs) with a network of locally hexagonally arranged through channels, 250−300 nm in diameter, were obtained by means of three-step anodization. The use of a short extra anodization step in acetone/$HClO_4$ has proven effective in breaking the Al_2O_3 barrier at the bottom of the channels, simplifying the formation of fully opened channels. Fe, Co, and Ni wires were electrochemically grown using the AAMs as templates. The easy axis of the three systems is along the wire axis due to their large shape anisotropy. The angular dependence of the coercivity indicates that due to the reduced shape anisotropy, owing to a smaller M_S, the Ni nanowires are more susceptible to dipolar interactions. The magnetization reversal mechanism for the Co system was successfully simulated by a curling mechanism.

Acknowledgment. This work was partially financed by the Catalan DGR (2001-SGR-00189) and the Spanish MEC (MAT-2004-01679 and MAT-2003-01052).

Note Added after ASAP Publication. There was an error in the labels of Figure 4 in addition to some minor textual errors in the version published ASAP February 25, 2005; the corrected version was published ASAP March 7, 2005.

CM047870Q